Food Sci Biotechnol (2017) 26(3):697–706
DOI 10.1007/s10068-017-0110-6

Effects of microwave-discharged cold plasma on synthesis and characteristics of citrate derivatives of corn starch granules

Hyun-Seok Kim[1] · Sea Cheol Min[2]

Received: 14 February 2017 / Revised: 22 February 2017 / Accepted: 27 February 2017 / Published online: 29 May 2017

Abstract The objectives of this study were to identify the potential function of microwave-discharged cold plasma (MCP) treatment in preparing starch citrate (SC) non-thermally and to investigate the physicochemical properties of MCP-induced starch citrates. SCs were prepared by either dry heating in a convection oven (as a reaction control; COV) or MCP treatment using N_2 (N_2-MCP) and N_2–O_2 (N_2/O_2-MCP). Fourier transform-infrared spectra of the MCP-induced SCs revealed new peaks indicating ester bonds. The molar degree of substation was 0.013–0.015 depending on the reaction conditions. The plasma-formed dents were observed more on the surfaces of granular starch citrates (GSCs) treated with N_2/O_2-MCP than N_2-MCP. Relative to COV, MCP-induced GSCs possessed lower resistant starch content, solubility, and gelatinization temperatures and higher swelling power. The pasting viscosities were higher with N_2-MCP GSCs and lower with N_2/O_2-MCP GSCs. The results suggest that MCP can be used as a novel catalyst for non-thermal starch citration.

Keywords Common corn starch · Starch citrate · Non-thermal starch citration · Cold plasma

✉ Sea Cheol Min
smin@swu.ac.kr

[1] Department of Food Science and Biotechnology, Kyonggi University, Suwon, Gyeonggi 16227, Korea

[2] Department of Food Science and Technology, Seoul Women's University, Seoul 01797, Korea

Introduction

Cold plasma (CP) was generated throughout gas excitation by means of corona discharge, dielectric barrier discharge, plasma jet, and microwave discharge without a significant increase in temperature in CP itself and the CP-treated materials [1, 2]. CP comprises activated and reactive chemical species (e.g., UV photons, electrons, free radicals, atomic oxygen, ozone, hydroxyl group, nitric oxide, and nitrogen dioxide) [1], which can function as initiators and/or promotors of various chemical reactions (e.g., covalent bond decomposition/formation, oxidation, amination, and esterification) [1, 11, 12]. There have been great interests in the application of CP treatment to the non-thermal sterilization of food [1–5] and the surface modification of packaging films made of synthetic and natural polymers [6–12]. The surface modification includes post-grafting functional monomers or natural polymers onto their active surface [11, 12]. In contrast to the research trends, few studies have studied in situ grafting of organic chemicals onto natural polymers by CP treatment [13]. Popescu et al. [13] successfully grafted both butyric and oleic acids to cellulose by CP treatment, suggesting that CP catalyzes the esterification between carboxylic acid groups of fatty acids and hydroxyl groups of cellulose. Consequently, CP may have great potential in acting as a non-toxic, eco-friendly catalyst in chemical modification of starch and non-starch polysaccharides with functional reagents.

Starch citrate has been considered or used as materials for removing heavy metal ions and/or organic matters from water waste [14], improving physical properties of biodegradable films [15, 16] and enhancing resistance of cotton or silk fabric against wrinkles [17]. In the field of food, it was reported that starch citrates prepared with citric

acid, a Generally Recognized as Safe-grade food additive did not exhibit pathological changes in mice during feeding [18, 19]. Also, the digestibility of starch citrates by pancreatin was inhibited with increasing their degree of substitution [19, 20]. Thus, citric acid has been considered as a safe, multifunctional reacting agent for substitution and cross-linking reaction of starches. Further, the citrate derivatives of starches can be a potential material to replace commercial resistant starches (RSs) synthesized with phosphorus oxychloride and sodium trimetaphosphate [18–20].

Citric acid (tricarboxylic acid) forms single and/or multiple ester bonds with starch molecules through condensation involving dehydration when heated over 120 °C for 1–7 h in a convection oven [19]. This traditional reaction induces higher contents of RS in starch citrates with increasing reaction temperature and time [19, 21]. However, the degree of browning also increases with reaction temperature and time [19, 21]. To enhance the reaction efficiency between citric acid and starch molecules during short reaction time (~1 h), a toxic reducing agent, sodium hypophosphite, is occasionally used [15]. Heating of starch-citric acid mixtures in a microwave oven is also applied as the reaction method [18], but requires considerable care due to their burning (or carbonization) from dramatic temperature increase. In addition, a lower RS content (2–8%, db) is obtained from microwave-assisted starch citrates [18] relative to those by the traditional reaction [19, 21]. Recently, an alternative method has been developed using a reactive extrusion technique [22, 23]. Although it can produce starch citrates with higher RS contents (up to 90%) within 1 h reaction time, their granular structure is destroyed due to higher shear from a concurrent rotating twin-screw extruder [22, 23]. Thus, the objective of this study was to investigate the effects of microwave-discharged CP (MCP) on the reactivities and physicochemical properties of starch citrates in granular state so as to design the non-thermal reaction process using CP as a non-toxic and eco-friendly catalyst for esterification between starch granules and citric acid.

Materials and methods

Materials

Normal corn starch (12.4% moisture, 24.3% amylose), a commercial product of Samyang Genex Co. (Seoul, Korea), was used as a starch source without additional purification. A total RS assay kit and anhydrous citric acid (CA) were purchased from Megazyme International Ltd. (Wicklow, Ireland) and Duksan Pure Chemicals Co., Ltd. (Ansan, Gyeonggi, Korea), respectively. All reagents and chemicals used in this study were of ACS grade.

Preparation of reaction mixtures

The reaction mixtures for GSCs were prepared according to the method of Kim and Kim [22]. CA was dissolved in deionized water (DIW), and then adjusted to pH 3.5 with 10 N NaOH. The CA concentrations were 10 and 20% on a dry starch weight basis (sb). Normal corn starch (1 kg, db) was mixed for 30 min at room temperature (~24 °C) with a CA solution (1 kg) using a mixer (5 L; Hobart Co., Troy, OH, USA). The mixture was transferred into a stainless-steel tray (36 × 32 × 6 cm^3) and dried at 50 °C using a forced convection oven (OF-G; Jeio Tech Co., Ltd., Daejeon, Korea) until its moisture content was <7.5%. The dried reaction mixtures were ground with a blender (HMF-3450S, Hanil Electric, Incheon, Korea), passed through a 50 mesh sieve (No. 50; Chunggye, Seoul, Korea), and stored in Teflon bottles at room temperature.

MCP treatment

The reaction mixtures were treated using MCP system (SWU-2; Seoul Women's University, Seoul, Korea) as outlined by Kim et al. [1] and Song et al. [3]. The reaction mixture (5 g) was evenly spread on a Teflon plate (16 cm diameter), which was placed in the treatment chamber of the MCP system. MCP treatment was conducted for 20 min at 900 W independently under N_2 (1 L/min, 0.7 kPa) and N_2–O_2 (80:20, v/v; 2.5 L/min, 1.3 kPa) environments, forming stable plasma. The surface temperature of the reaction mixtures was ~32 °C during treatment according to the measurement using an infrared thermometer (DT 44L; DIAS Infrared GmbH, Dresden, Germany). For a reaction control (COV in Table 1) of MCP treatments (LPaG1-2 and LPbG1-2 in Table 1), the reaction mixture (20 g, db) prepared with 10% CA was dry-heated for 60 min at 135 °C in a convection oven (FO-600 M; Jeio Tech Co., Ltd., Daejeon, Korea) [24]. MCP-treated and dry heat-treated reaction mixtures were washed three times with 50% (v/v) aqueous ethanol and then once with absolute ethanol to remove the unreactive CA, and dried at 45 °C for 24 h [22]. The reaction conditions for preparing GSCs are presented in Table 1. LPaG1-2 and LPbG1-2 are the starch citrates treated by MCP under the different gas environments of N_2 alone and the mixture of N_2 and O_2 (80:20, v/v), respectively. Also, LPaG1 and LPaG2 (or LPbG1 and LPbG2) refer to the starch citrates prepared by MCP treatment using the reaction mixtures with different CA concentrations of 10 and 20% (sb).

Table 1 Reaction conditions for the synthesis of granular starch citrates by dry heat and microwave-discharged cold plasma treatments

Treatment	CA (%, s.b)	pH	T (°C)	t (min)	Gas composition (%, v/v)		E (W)
					N_2	O_2	
Native	–	–	–	–	–	–	–
COV	10	3.5	135	60	–	–	–
LPaG1	10	3.5	32	20	100	–	900
LPaG2	20	3.5	32	20	100	–	900
LPbG1	10	3.5	32	20	80	20	900
LPbG2	20	3.5	32	20	80	20	900

CA, anhydrous citric acid; T, temperature; t, time; E, electric power; COV, granular starch citrate prepared through dry heat treatment in a convection oven; LPaG1-2 and LPbG1-2, granular starch citrates prepared through microwave-discharged cold plasma treatment

Morphology

Starch samples were viewed at 1200 times magnification with a field-emission scanning electron microscope (FE-SEM, JSM-6700F; Jeol Ltd., Tokyo, Japan) following the method of Kim and Kim [25].

Fourier transform-infrared spectroscopy (FT-IR)

FT-IR spectra of starch samples were obtained using Spectrum One System (Perkin-Elmer, Waltham, MA, USA). The tablets prepared from the starch sample and potassium bromide (FT-IR grade, >99%; Sigma-Aldrich Co., St. Louis, MO, USA) were scanned at the wavelength range of 400–4000 cm^{-1} with a resolution of 4 cm^{-1} [22].

Molar degree of substitution (MS)

CA bound to GSCs was quantified according to the method outlined by Kim and Kim [24]. MS was calculated as the ratio of moles of anhydrous CA to that of anhydroglucose units of starch.

X-ray diffraction (XRD)

XRD patterns of starch samples were investigated with an X-ray diffractometer (D8 Advance; Bruker AXS GmbH, Karlsruhe, Germany), following the method of Shin et al. [26]. The relative crystallinity (RC) was calculated as the percent ratio of the difference in the diffractogram area between granular and amorphous starches to the diffractogram area of granular starches [27]. An amorphous starch was prepared through autoclaving-cooling treatment with native starch [28].

RS content

The GSC paste was prepared by mixing GSC (100 mg, db) with DIW (4 mL), and heating for 30 min in a boiling water bath, followed by cooling to 37 °C [24]. The RS contents of GSC and GSC paste were determined using a total RS assay kit (Megazyme International Ltd., Wicklow, Ireland) according to the Approved Method 32-40 [29].

Swelling power (SP) and solubility

The SP of the starch samples was measured at 75 °C according to the method outlined by Shin et al. [26]. SP was defined as the ratio of weights of the swollen GSC to the initial counterpart. For solubility, the total sugar contents in the supernatant recovered from SP measurement were measured by a sulfuric acid-phenol method [30]. Solubility was defined as the percent (%) ratio of weights of total sugar (converted into starch) in the supernatant to the initial starch samples.

Differential scanning calorimetry (DSC)

Gelatinization property of starch samples was investigated with DSC (Q2000; TA Instruments, New Castle, DE, USA). A starch sample (5 mg, db) was weighed into aluminum pans, and DIW was added to a total weight of 20 mg, followed by hermetical sealing. The pan was held overnight at room temperature (24 °C) for equilibrium, after which it was scanned from 20 to 100 °C at a heating rate of 5 °C. The empty pan was used as the Ref. [26].

Rapid visco analyzer (RVA)

Pasting viscosity profiles of starch samples were investigated with RVA (RVA-3D; Newport Scientific, NSW, Australia). The starch sample (2.0 g, db) was directly weighed into an aluminum canister, and DIW was added to a total weight of 28 g. The starch slurry was manually stirred for 30 s with a spatula and plastic paddle, followed by its insertion into RVA. The rotation speed of the plastic paddle was maintained at 160 rpm over the programmed temperature profile: holding at 50 °C for 1 min, heating

from 50 to 95 °C at a heating rate of 12 °C/min, holding at 95 °C for 2.5 min, cooling to 50 °C at a cooling rate of 12 °C/min, and holding at 50 °C for 2 min.

Statistical analysis

GSC preparation was repeated three times according to the reaction conditions (Table 1), and all measurements were repeated three times for analysis. All experimental data were analyzed using one-way ANOVA and expressed as mean ± standard deviation. Significant differences in characteristics among treatments were analyzed with Tukey's HSD test at $p < 0.05$. All statistical analyses were conducted with Minitab 16 (Minitab Inc., State College, PA, USA).

Results and discussion

FT-IR

FT-IR spectra of native starch and reaction mixtures treated by MCP were investigated to verify if the esterification between starch molecule (ST) and CA occurred under MCP (Fig. 1). The well-known starch citrate (SC; COV in Table 1) prepared by dry heating in a convection oven was used as a reaction control of MCP-treated reaction mixtures [21–24]. A typical FT-IR spectrum was obtained for native starch, consistent with that reported in literature [21–24]. Similar to COV, the reaction mixtures treated with MCP revealed a new peak generated from the stretching vibration of carbonyl groups in ester bonds at the wavelength range of 1710–1760 cm^{-1} (Fig. 1 arrows) [15, 16, 21–24]. Consequently, MCP appeared to catalyze the formation of ester bonds between ST and CA, which could synthesize SC in a non-thermal manner.

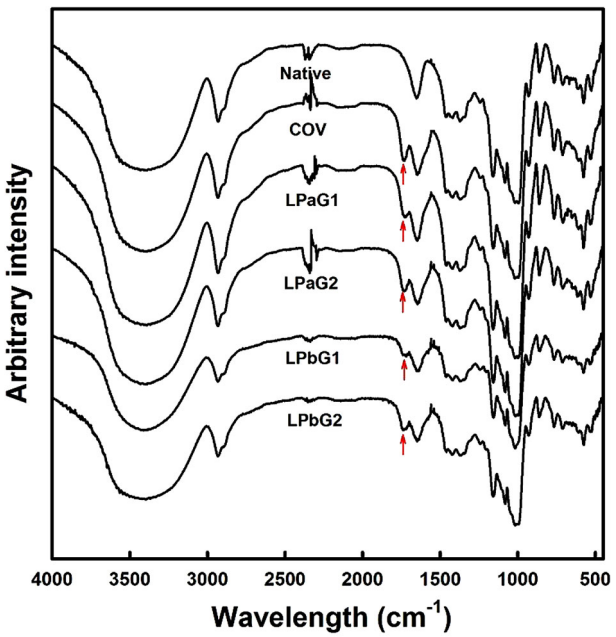

Fig. 1 FT-IR spectra of native starch and granular starch citrates prepared by dry heat (COV) and microwave-induced cold plasma (LPaG1-2 and LPbG1-2) treatments. See Table 1 for the detailed reaction conditions

MS

The reactivity of COV and MCP-induced SC was assessed with their respective MS (Table 2). In general, the MS of SC prepared by dry heating in a convection oven increased with reaction temperature and time at a given CA concentration [14, 18, 19, 23, 24]. Nevertheless, for comparison of the reaction efficiency of MCP treatment that was completed within 20 min to that of a traditional reaction, the reaction mixture for COV was dry-heated at 135 °C only for 60 min (a minimal reaction time to form ester bonds between ST and CA over 120 °C). The MS of COV was 0.016, compatible with that of SC prepared under reaction conditions identical to those in this study [23]. Accordingly, the method adopted in this study to determine the MS of SC was appropriate for investigating the reactivity of MCP-induced SCs. For MCP-induced SCs (LPaG1-2 and LPbG1-2), MS ranged from 0.012 to 0.015 and was slightly lower (but statistically significant) than that of COV (Table 2). Within a given CA concentration, SCs treated with MCP by N_2 (N_2-MCP) exhibited slightly lower MS than those with MCP by N_2–O_2 (N_2/O_2-MCP) (not significant for LPaG1 vs. LPbG1; statistically significant for LPaG2 vs. LPbG2) (Table 2). Despite minute differences in the MS of SCs between N_2-MCP and N_2/O_2-MCP treatments, N_2/O_2-MCP (relative to N_2-MCP) may be more effective for dehydrogenation and dehydroxylation of STs and CA due to the presence of oxygen atom, hydroxyl group, and ozone in N_2/O_2-MCP [9, 13]. For a given MCP-forming gas, the difference in the MS of SCs was 0.001 for LPaG1 vs. LPaG2 and 0.002 for LPbG1 versus LPbG2 (Table 2), suggesting that the MS of MCP-induced SCs was less dependent on CA concentration. Oh et al. [5] noted CP-affected polymer films to be 10 nm or less in depth, which implies that MCP catalyzed the reaction of ST with CA at their periphery.

Morphology

The morphological characteristics of native starch and SCs were observed with FE-SEM, and shown in Fig. 2. Native starches exhibited polygonal and round shapes with smooth surfaces (Fig. 2 Native), as commonly reported in literature [21, 23]. Although COV (reacted in a convection oven as a

Table 2 Mean[a] values for molar degree of substitution (MS), resistant starch (RS) content, solubility, swelling power (SP), relative crystallinity (RC), and gelatinization of native starch and granular starch citrates

Treatment	MS	RC (%)	RS (%, d.b)		Solubility (%, d.b)	SP (g/g)	T_o^b (°C)	T_p^b (°C)	T_c^b (°C)	ΔH^b (J/g)
			Uncooked	Cooked						
Native	–	26.1 ± 0.1[a]	6.1 ± 0.2[e]	N/D[c]	5.6 ± 0.3[e]	10.1 ± 0.2[e]	64.9 ± 0.1[c]	69.9 ± 0.0[e]	73.8 ± 0.1[c]	10.5 ± 0.5[a]
COV[d]	0.016 ± 0.000[a]	26.1 ± 0.2[a]	21.6 ± 0.5[a]	18.8 ± 0.1[a]	16.8 ± 0.1[a]	10.8 ± 0.1[d]	65.7 ± 0.0[a]	72.5 ± 0.7[a]	84.2 ± 4.1[a]	10.9 ± 0.2[a]
LPaG1[d]	0.012 ± 0.001[c]	26.1 ± 0.0[a]	12.9 ± 0.1[c]	10.5 ± 0.5[c]	12.7 ± 0.1[b]	12.1 ± 0.3[a]	65.3 ± 0.1[b]	70.1 ± 0.1[b]	74.1 ± 0.2[b]	10.5 ± 0.0[ab]
LPaG2[d]	0.013 ± 0.000[c]	26.1 ± 0.1[a]	13.0 ± 0.3[c]	12.3 ± 0.3[b]	7.4 ± 0.6[d]	11.6 ± 0.1[b]	64.4 ± 0.1[d]	69.7 ± 0.2[cd]	73.8 ± 0.2[bc]	10.5 ± 0.0[ab]
LPbG1[d]	0.013 ± 0.001[c]	26.1 ± 0.0[a]	11.5 ± 0.3[d]	10.3 ± 0.5[c]	12.6 ± 0.1[b]	11.6 ± 0.1[b]	64.3 ± 0.2[d]	69.6 ± 0.2[cd]	73.8 ± 0.5[bc]	10.5 ± 0.3[a]
LPbG2[d]	0.015 ± 0.000[b]	26.1 ± 0.1[a]	14.7 ± 0.2[b]	11.9 ± 0.3[b]	8.9 ± 0.4[c]	11.1 ± 0.1[c]	64.1 ± 0.3[d]	69.4 ± 0.2[cd]	73.7 ± 0.1[c]	10.0 ± 0.7[ab]

[a] Mean values of three replicate measurements; values sharing the same lowercase letters within a column are not significantly different at $p < 0.05$

[b] T_o, T_p, and T_c indicate gelatinization onset, peak, and completion temperatures, respectively; ΔH refers to gelatinization enthalpy

[c] Not detected

[d] COV, LPaG1-2, and LPbG1-2 indicate the granular starch citrates prepared through the dry heat and microwave-discharged cold plasma treatments, respectively. The detailed reaction conditions for granular starch citrates are depicted in Table 1

reaction control) showed granular shapes similar to those of native starch, it revealed rough and rugged surfaces. The particulated and truncated granule fragments were also frequently viewed (COV in Fig. 2). Similar results were reported by Xie et al. [21], Kim and Kim [22], and Kim [23]. Kim [23] suggested that the distorted and disrupted granule structures, as observed in this study, are due to re-aggregation and collapse of SCs thermally damaged by hot melt of CA in the reaction mixture exposed at high temperatures. However, SCs non-thermally treated with MCP (LPaG1-2 and LPbG1-2 in Fig. 2) exhibited the granular structures generally similar to those observed in native starch, although some granules possessed dents distributed on their surfaces (Fig. 2 arrows). Pankaj et al. [7] suggested that the bombardment of energetic plasma species such as electrons, radicals, and UV protons can etch on the surface of high amylose corn starch film, resulting in an increase in its roughness. Accordingly, the dent structures observed in this study may be attributed to the collision of energetic species within MCP on the surfaces of GSCs. Furthermore, the granules with dents were more observed in LPbG1-2 relative to LPaG1-2 (Fig. 2 arrows). Inagaki et al. [31] demonstrated that the effect of CP etching on a PE film was influenced by the types of plasma-forming gases, and increased in the order $O_2 > H_2 > N_2 > Ar$. In this study, thus, the more frequent dents of LPbG1 and LPbG2 may be due to the potential presence of reactive oxygen species in N_2/O_2-MCP (Table 1).

XRD

XRD patterns and RC of native starch and GSCs by dry heating (COV) and MCP treatment (LPaG1-2 and LPbG1-2) were investigated to identify macrostructural changes in GSCs treated with MCP (Fig. 3(A), Table 2). Native starch and COV revealed major peaks at 15.2°, 17.3°, 17.1°, and 18.0°, which explained the typical A-type crystal packing arrangement within starch granules [23]. Their XRD patterns did not exhibit significant shifts in major peaks or changes in overall intensities of X-ray diffractograms (Fig. 3(A)). In addition, the RC (calculated from the X-ray diffactograms) did not significantly differ between native starch and COV (Table 2). The noted results were in good agreement with those of Kim [23], who reported no differences in XRD patterns and RC between native starch and SC dry-heated at 150 °C for 60 min. On the other hand, both XRD patterns and RCs of MCP-induced GSCs were not different from those of native starch and COV (Fig. 3(A); Table 2). Pankaj et al. [7] suggested that oxygenation of the high amylose corn starch film by CP treatment facilitates hydrogen bonding among starch molecules and/or double helices within its crystals, resulting in its RC increase. In this study, MCP may be

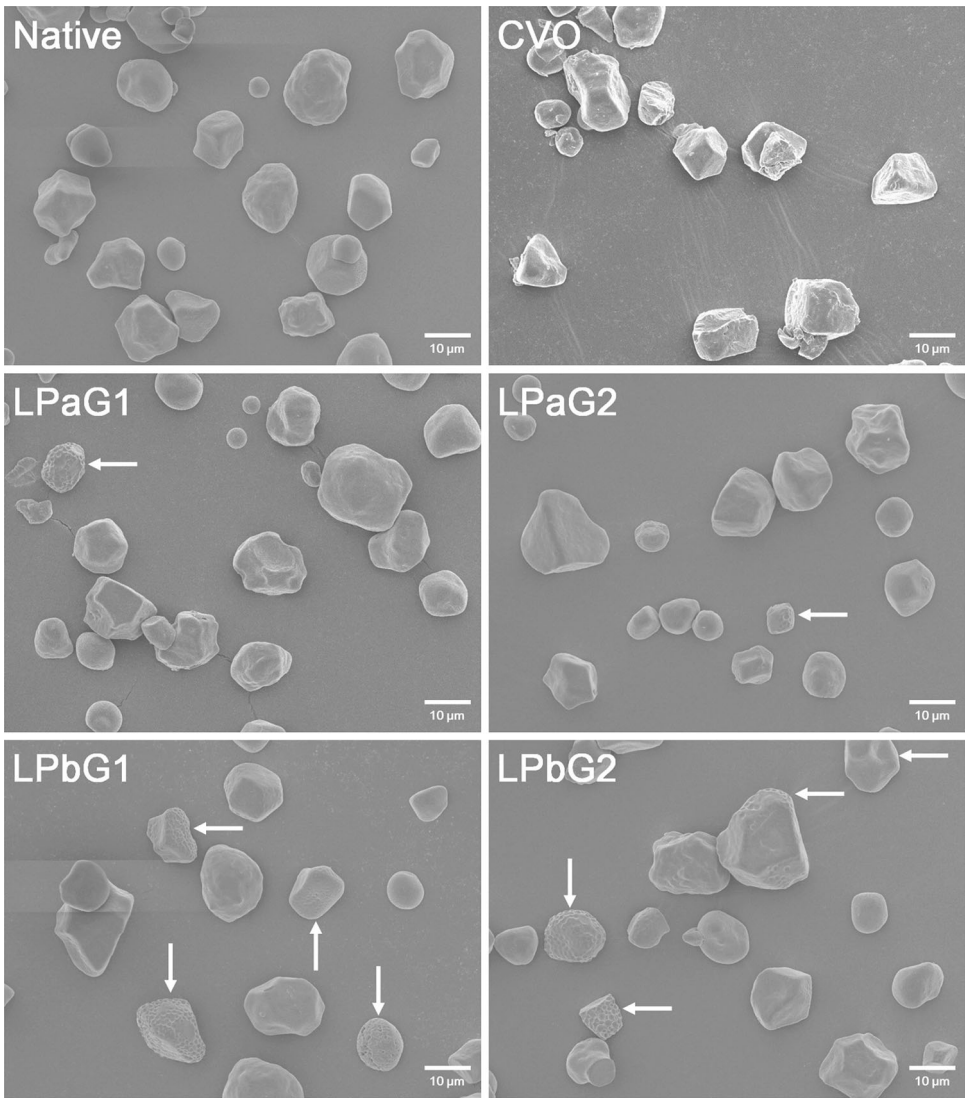

Fig. 2 FE-SEM images of native starch and granular starch citrates prepared by dry heat (COV) and microwave-induced cold plasma (LPaG1-2 and LPbG1-2) treatments (*scale bar* 10 μm). See Table 1 for detailed reaction conditions

impossible to infiltrate into GSC granules as supported by previous suggestion that it acts at their periphery. The results suggest that MCP did not affect amylopectin double helices and/or clusters (responsible for starch crystal structure) of their interior, leading to no changes in their XRD patterns and RCs.

RS content

Resistance of native starch and GSCs to amylolytic enzymes was assessed with their RS contents (Table 2). In uncooked state, all GSCs (11.5–21.6%) exhibited significantly higher RS contents than native starch (6.1%). It was consistent with previous reports that bulky CA groups within SCs restricted attack or action of amylolytic enzymes to ST [18, 19, 23]. For GSCs, the RS contents of MCP-induced GSCs (11.5–14.7%) were significantly lower than that of COV (21.6%). The noted differences in RS contents may be a result of the deviation in MS among GSCs, because RS contents of SCs were positively correlated with their MS [19, 24]. Within a given MCP-forming gas, MCP-induced GSCs appeared to follow the general relationship between RS content and MS of SCs, as mentioned above (Table 2). However, in the case of LPaG1 and LPbG1 treated with N_2-MCP and N_2/O_2-MCP, respectively, the RS content was significantly lower in LPbG1 relative to LPaG1, even though both possessed similar MS (Table 2). This finding may result from the partial scission of ST throughout plasma oxidation by active oxygen species in N_2/O_2-MCP [12]. On the other hand, there is a report that activated surfaces of the defatted soybean meal-based film by CP treatment may be partially restored to its untreated state during storage [5], implying instability of CP-induced activation effects. To examine the stability of MCP-induced ester bonds between ST and CA, aqueous suspensions of GSCs were cooked in a hot water bath,

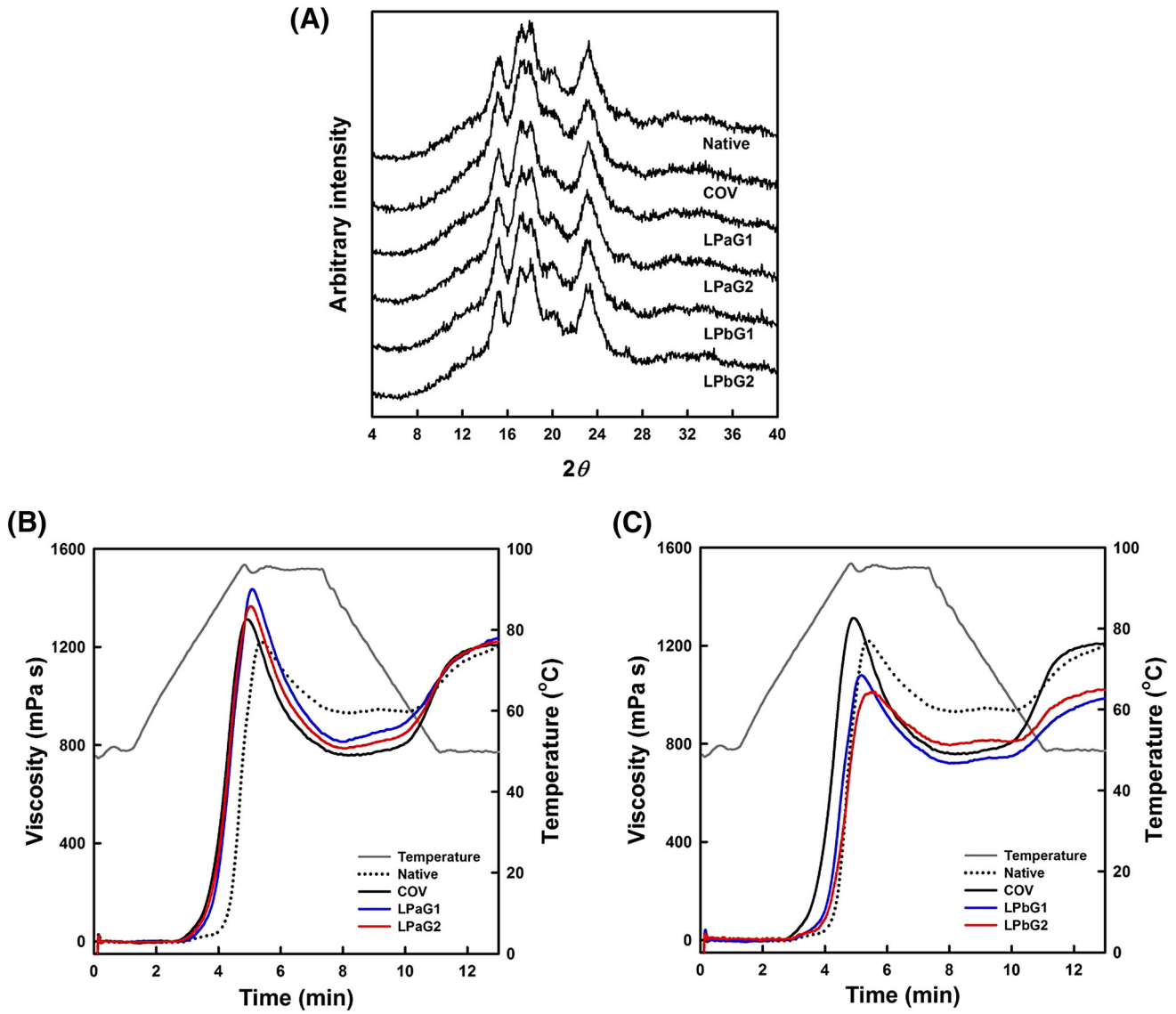

Fig. 3 XRD patterns (**A**) and pasting viscosity profiles (**B**, **C**) of native starch and granular starch citrates prepared by dry heat (COV) and microwave-induced cold plasma (LPaG1-2 and LPbG1-2) treatments. See Table 1 for detailed reaction conditions

followed by determination of their RS contents (Table 2). The deviation in RS content between uncooked and cooked GSCs was 2.8% points for COV and 0.7–2.8% points for MCP-induced GSCs (Table 2). More thermally stable ester bonds might be formed by MCP (relative to dry heating) treatment.

Solubility and SP

The solubility and SP of native starch and GSCs were determined at 75 °C (Table 2). The solubility and SP were significantly higher for GSCs (7.4–16.8% and 10.8–12.1 g/g, respectively) relative to native starch (5.6% and 10.1 g/g, respectively) (Table 2). Both solubility and SP of SCs were much lower than those of their respective untreated (native) starches in the case that ST within SCs was primarily cross-linked (relative to substituted) with CA [23]. Thus, COV and MCP-induced GSCs in this study may be formed mainly by substitution (single esterification) of ST with CA, although there may still be cross-linking among starch molecules by CA [19] to lesser extents. Within GSCs, COV revealed higher solubility than MCP-induced GSCs, while slightly higher (but statistically significant) SP was obtained for MCP-induced GSCs (relative to COV) (Table 2). Assuming that ST was substituted with CA only by single esterification, COV with the highest MS should have revealed higher solubility and SP than MSP-induced GSCs [23]. However, in this study, the smallest SP was found for COV among GSCs. Both substitution and cross-linking reaction were known to simultaneously occur in

starch citration [19, 23], although their relative frequency could be different depending on the reaction conditions. As mentioned above, mono-starch mono-citrate (MSMC; by substitution) may be much more dominant within all GSCs than di-starch mono-citrate (DSMC; by cross-linking), based on comparison between the solubility and SP of GSCs to those of native starch. The highest MS of COV likely possessed the highest contents of MSMC and DSMC relative to other GSCs, which might result in restriction of its swelling due to its relatively high DSMC. On the other hand, MSP-induced GSCs did not follow the common trend that the solubility and SP of SCs increased (dominant for substitution) or decreased (dominant for cross-linking) with increasing MS [18, 19, 23]. For example, LPaG2 revealed lower solubility and higher SP than LPbG1, even though they possessed the same MS (0.013). Accordingly, the solubility and SP of MCP-induced GSCs were contradictory to general trends in starch citration and may not be appropriately interpreted with the experimental results provided in this study.

DSC

The gelatinization properties of native starch and GSCs were investigated with DSC, and exhibited in Table 2. Relative to native starch, gelatinization onset, peak, and completion temperatures of COV shifted toward high temperature (Table 2). This result implies that citration reaction (substitution and cross-linking) by dry heating occurred on the surfaces as well as in the internal matrices of starch granules, enhancing their resistance to thermal melting [23]. However, the gelatinization temperatures of MCP-induced GSCs, regardless of CA concentration and MCP-forming gas, were commonly similar to those of native starch, although there were minute differences in their gelatinization temperatures (Table 2). It may further support that MCP functions only at the peripheries of starch granules, as previously suggested. On the other hand, the gelatinization enthalpies (10.0–10.9 J/g) did not significantly differ for native starch, COV, and MCP-induced GSCs, as supported by their XRD patterns and RC that were not significantly changed according to the reaction conditions (Fig. 3(A), Table 2). Consequently, MCP treatment did not affect the granule stability, crystal formation, and crystalline perfection of starches.

Pasting viscosity

Pasting viscosity profiles and characteristics of native starch, COV, and MCP-induced GSCs were investigated and are presented in Fig. 3(B, C) and Table 3, respectively. Their pasting viscosity profiles were typical, as observed for native and modified starches [23], although there were differences in the levels of pasting viscosity among them (Fig. 3(B), (C)). Compared to the pasting viscosity profile of native starch, COV began to rapidly develop its pasting viscosity (lower pasting temperature) and exhibited higher peak, lower trough, and similar final viscosities (Fig. 3(B), (C)), resulting in higher breakdown and setback viscosities (Table 3). The noted trends in pasting viscosity were found for relatively lower MS of SCs, which were more frequently substituted than cross-linked [18, 23, 24]. The pasting viscosity profiles of LPaG1 and LPaG2 treated with N_2-MCP were similar to the profile of COV, but higher at all points over the programmed temperature profile (Fig. 3(B)). Due to the differences in their pasting viscosity profiles, LPaG1 and LPaG2 revealed higher peak, trough, and final viscosities, causing higher breakdown and lower setback viscosities (Table 3). The observed phenomena were opposite to those of substituted starches, whose pasting viscosities increased with their MS [32]. It can be explained by the previously mentioned suggestion that relative frequency of DSMC is higher for COV than MCP-induced GSCs due to their relative differences in MS. Further, LPaG1 showed higher pasting viscosities (except for setback viscosity) than LPaG2 (Fig. 3(B); Table 3), which may be explained by the fact that LPaG1 possessed higher solubility and SP than LPaG2 (Table 2). On the other hand, for LPbG1 and LPbG2 treated with N_2/O_2-MCP, the pasting viscosity profiles were lower at all and partial points (relative to native starch and COV, respectively) over the programmed temperature profile (Fig. 3(C)). Their pasting viscosity development was faster than native starch, but later than COV (Table 3), as the results of differences in MS between MCP-induced GSCs and either native starch or COV (Table 2). Moreover, their peak, trough (except for LPbG2), breakdown, final, and setback viscosities were lower than those of COV (Table 3). The observed phenomena may not be explained by differences in either MS or solubility and SP among them depicted in Table 2, due to inconsistency in general patterns observed for lower MS of SCs [18, 23, 24] and hydroxypropylated starches [32]. Based on their lower solubilities (Table 2), their reduced pasting viscosities may not result from the partial hydrolysis of starch granules by CA during preparation of the reaction mixture [33] and plasma oxidation [12] during MCP treatment. The most possible explanation might be the reduction of swollen granule rigidity of LPbG1 and LPbG2 (treated by N_2/O_2-MCP) against continued shear. As shown in this study (Fig. 2 LPbG1-2), the more dents (likely damaged by bombardment of reactive oxygen species within MCP) on the surfaces of LPbG1 and LPbG2 granules than others might weaken their granule integrity, resulting in rupturing their swollen granules before arrival at maximum granule swelling by continued shear during RVA analysis. The

Table 3 Mean[a] values for pasting viscosity characteristics of native starch and granular starch citrates

Treatment	T_p^b (°C)	Pasting viscosity (mPa s)				
		Peak	Trough	Breakdown	Final	Setback
Native	90.1 ± 0.6[a]	1221.5 ± 2.1[d]	936.5 ± 2.1[a]	285.0 ± 0.0[e]	1201.0 ± 8.5[c]	264.5 ± 6.4[d]
COV[c]	80.9 ± 0.0[f]	1318.5 ± 9.2[c]	761.0 ± 5.7[d]	557.5 ± 3.5[c]	1220.0 ± 7.1[ab]	459.0 ± 1.4[a]
LPaG1[c]	83.6 ± 0.5[d]	1435.0 ± 8.5[a]	817.0 ± 5.7[b]	618.0 ± 2.8[a]	1238.0 ± 9.9[a]	421.0 ± 4.2[c]
LPaG2[c]	81.7 ± 0.4[e]	1371.9 ± 9.4[b]	793.4 ± 8.7[c]	578.5 ± 0.6[b]	1231.5 ± 9.2[a]	438.1 ± 0.5[b]
LPbG1[c]	85.2 ± 0.4[c]	1083.5 ± 6.4[e]	725.0 ± 5.7[e]	358.5 ± 0.7[d]	989.3 ± 3.9[d]	264.3 ± 1.8[d]
LPbG2[c]	86.9 ± 0.6[b]	1019.0 ± 8.5[f]	802.0 ± 9.9[c]	217.0 ± 1.4[f]	1027.5 ± 9.2[a]	225.5 ± 0.7[e]

[a] Mean values of three replicate measurements; Values sharing the same lowercase letters within a column are not significantly different at $p < 0.05$

[b] Pasting temperature

[c] COV, LPaG1-2, and LPbG1-2 indicate the granular starch citrates prepared through the dry heat and microwave-discharged cold plasma treatments, respectively. The detailed reaction conditions for granular starch citrates are depicted in Table 1

results indicate that pasting viscosities decreased in LPbG1 and LPbG2. Kim and Kim [22] suggested that the structural damage of SC granules reduced their pasting viscosity.

In conclusion, this study demonstrated the physicochemical properties of SCs non-thermally prepared by MCP treatment. Overall results revealed that MCP successfully esterified ST with CA, and MCP-induced GSCs (relative to native starch) altered their physicochemical properties, similar to those of SC prepared by a traditional reaction method. Thus, MCP would possess great potential for functioning as a novel catalyst in in situ non-thermal grafting of CAs on starch molecules. Nevertheless, it is likely that overcoming the limitation of CP, which has a narrow penetrating depth of the matters, will be an important area of future research to enhance the reaction efficiency of MCP treatment.

Acknowledgements This work was supported by a research grant from Seoul Women's University (2017) and Basic Science Research Program of the National Research Foundation of Korea (NRF), which was funded by the Ministry of Education (NRF-2015R1D1A3A01019510).

Compliance with ethical standards

Conflict of interest The authors declare no conflict of interest.

References

1. Kim JE, Lee DU, Min SC. Microbial decontamination of red pepper powder by cold plasma. Food Microbiol. 38: 128–136 (2014)
2. Kim JE, Oh YJ, Won MY, Lee KS, Min SC. Microbial decontamination of onion powder using microwave-powered cold plasma treatments. Food Microbiol. 62: 112–123 (2017)
3. Song AY, Oh YJ, Kim EJ, Song KB, Oh DH, Min SC. Cold plasma treatment for microbial safety and preservation of fresh lettuce. Food Sci. Biotechnol. 24: 1717–1724 (2015)
4. Lee H, Kim JE, Chung MS, Min SC. Cold plasma treatment for the microbiological safety of cabbage, lettuce, and dried figs. Food Microbiol. 51: 74–82 (2015)
5. Oh YA, Roh SH, Min SC. Cold plasma treatments for improvement of the applicability of defatted soybean meal-based edible film in food packaging. Food Hydrocolloid. 58: 150–159 (2016)
6. Pankaj SK, Bueno-Ferrer C, Misra NN, Bourke P, Cullen PJ. Zein film: Effects of dielectric barrier discharge atmospheric cold plasma. J. Appl. Polym. Sci. 131: 40803–40808 (2014)
7. Pankaj SK, Bueno-Ferrer C, Misra NN, O'Neill L, Tiwari BK, Bourke P, Cullen PJ. Dielectric barrier discharge atmospheric air plasma treatment of high amylose corn starch films. LWT Food Sci. Technol. 63: 1076–1082 (2015)
8. Pankaj SK, Bueno-Ferrer C, Misra NN, O'Neill L, Tiwari BK, Bourke P, Cullen PJ. Physicochemical characterization of plasma-treated sodium caseinate film. Food Res. Int. 66: 438–444 (2014)
9. De Geyter N, Morent R, Leys C, Gengembre L, Payen E. Treatment of polymer films with a dielectric barrier discharge in air, helium, and argon at medium pressure. Surf. Coat. Tech. 201: 7066–7075 (2007)
10. De Geyter N, Morent R, Desmet T, Trentesaux M, Gengembre L, Dubruel P, Leys C, Payen E. Plasma modification of polylactic acid in a medium pressure DBD. Surf. Coat. Tech. 204: 3272–3279 (2010)
11. Poncin-Epaillard F, Chevet Bruno, Brosse JC. Modification of isotactic polypropylene by a cold plasma or an electron beam and grafting of the acrylic acid onto these activated polymers. J. Appl. Polym. Sci. 53: 1291–1306 (1994)
12. Theapsak S, Watthanaphanit A, Rujiravanit R. Preparation of chitosan-coated polyethylene packaging films by DBD plasma treatment. ACS Appl. Mater. Inter. 4: 2474–2482 (2012)
13. Popescu MC, Totolin M, Tibirna CM, Sdrobis A, Stevanovic T, Vasile C. Grafting of softwood kraft pulps fibers with fatty acids under cold plasma conditions. Int. J. Biol. Macromol. 48: 326–335 (2011)
14. Wing RE. Starch citrates: Preparation and ion exchange properties. Starch-Stärke 51: 354–361 (1996)
15. Reddy N, Yang Y. Citric acid cross-linking of starch films. Food Chem. 118: 702–711 (2010)
16. Ma X, Jian R, Chang RR, Yu J. Fabrication and characterization of citric acid-modified starch nanoparticles/plasticized starch composites. Biomacromolecules 9: 3314–3320 (2008)

17. Yang CQ, Wang X, Kang I. Ester cross-linking of cotton fabric by polymeric carboxylic acids and citric acid. Text Res. J. 67: 334–342 (1997)
18. Jyothi AN, Moorthy SN, Sreekumar JN, Rajasekharan KN. Studies on the properties of citrate derivatives of cassava (*Manihot esculenta* Crantz) starch synthesized by microwave technique. J. Sci. Food Agr. 87: 871–879 (2007)
19. Xie X, Liu Q. Development and physicochemical characterization of new resistant starch from different corn starches. Starch-Stärke 56: 364–370 (2004)
20. Wepner B, Berghofer E, Miesenberger E, Tiefenbacher K, Ng PNK. Citrate starch-application as resistant starch in different food systems. Starch-Stärke 51: 354–361 (1999)
21. Xie X, Liu Q, Cui SW. Studies on the granular structure of resistant starches (type 4) from normal, high amylose and waxy corn starch citrates. Food Res. Int. 39: 332–341 (2006)
22. Kim SH, Kim HS. Impact of reactive extrusion parameters on the resistant contents and pasting properties of starch citrates. Food Eng. Prog. 19: 193–200 (2015)
23. Kim SH. Development of digestion-resistant citric acid cross-linked starch by continuous-circulating heating reactor. MS thesis, Andong National University, Andong, Gyeongsangbuk, Korea (2014)
24. Kim SH, Kim HS. Influence of semi-dry heating reaction conditions on resistant starch contents and pasting viscosities of starch citrates. Food Eng. Prog. 19: 313–319 (2015)
25. Kim EJ, Kim HS. Influence of pectinase treatment on the physicochemical properties of potato flours. Food Chem. 167: 425–432 (2015)
26. Shin EH, Baik MY, Kim HS. Comparison of physicochemical properties of starches and parenchyma cells isolated from potatoes cultivated in Korea. Food Sci. Biotechnol. 24: 955–963 (2015)
27. Cheetham NWH, Tao L. Variation in crystalline type with amylose content in maize starch granules: An X-ray powder diffraction study. Carbohyd. Polm. 36: 277–284 (1998)
28. Kim BS, Kim HS, Hong JS, Huber KC, Shim JH, Yoo SH. Effects of amylosucrase treatment on molecular structure and digestion resistance of pre-gelatinised rice and barley starches. Food Chem. 138: 966–975 (2013)
29. AACC. Approved Method of the AACC. 10th ed. Method 32-40. American Association of Cereal Chemists, St. Paul, MN, USA (2000)
30. Dubois M, Gilles KA, Hamilton JK, Rebers PA, Smith F. Colorimetric method for determination of sugars and related substances. Anal. Chem. 28: 350–356 (1956)
31. Inagaki N, Narushim K, Tuchida N, Miyazak K. Surface characterization of plasma-modified poly(ethylene terephthalate) film surfaces. J. Polym. Sci. Pol. Phys. 42: 3727–3740 (2004)
32. Kim HS, Huber KC. 2010. Impact of A/B-type granule ratio on reactivity, swelling, gelatinization, and pasting properties of modified wheat starch. Part I: Hydoxypropylation. Carbohyd. Polym. 80: 94–104 (2010)
33. Chung HJ, Jeong HY, Lim ST. Effects of acid hydrolysis and defatting on crystallinity and pasting properties of freeze-thawed high amylose corn starch. Carbohyd. Polym. 54: 449–455 (2003)